Ecological Modelling 467 (2022) 109931

Contents lists available at ScienceDirect

Ecological Modelling

journal homepage: www.elsevier.com/locate/ecolmodel

Harmful algal bloom dynamics in a tidal river influenced by hydraulic control structures

Jaeyoung Kim[a], Dongil Seo[a,*], John R. Jones[b]

[a] Department of Environmental Engineering, Chungnam National University, 99, Daehak-ro, Yuseong-gu, Daejeon, 341342, Republic of Korea

[b] School of Natural Resources, University of Missouri, 103 Anheuser-Busch Natural Resources Building, Columbia, MO 65211, United States of America

ARTICLE INFO

Keywords:
Harmful algal blooms
Cyanobacteria
The Han river
The Singok weir
Flow regulating structure
EFDC

ABSTRACT

The Singok weir, an instream structure in the Han River estuary constructed in the 1980s for multiple purposes, has interfered with natural river flow. Removal of this structure has been considered to restore water quality, including reducing algal blooms. Spatiotemporal changes in water quality, hydrodynamics, hydrology, and algal growth resulting from the removal of the Singok weir were analyzed using 3-D hydrodynamic, water quality, and sediment transport modules in the Environmental Fluid Dynamics Code model for a five-year period (2013 ∼ 2017) with field data. Weir removal decreased water depth and thus water volume by >10%, which increased average nutrient concentrations given fixed pollutant inputs. With the weir removal, average cyanobacteria decreased in the upper region during summer but increased in the lower region. However, differences in cyanobacteria biomass were less than 1.0 mg Chl-a/m^3 except during 2015, the driest summer, where peak cyanobacteria increased by 20% (11.8 mg/m^3). Factors limiting summer algal growth tended to increase modestly during normal flow (<3.1%), which suggests the weir removal can potentially enhance algal growth. The role of hydrology stood out as the major factor determining algal growth, with greater relative importance than nutrients, light, and temperature. Simulations showed minimum discharge of 150 m^3/s from the Paldang dam was required to avoid excessive cyanobacteria growth downstream. Hydraulic residence time during summer determined the growth potential of algae; low discharge provided sufficient residence time for algae to proliferate, and conversely. This result also emphasizes the importance of seasonal and hydrodynamic assessments when analyzing cyanobacteria in response to external changes, which can be masked in annual average values by numerous factors.

1. Introduction

Harmful algal blooms (HABs), dominated by cyanobacteria, occur in response to high nutrient concentrations and are considered a common surface water quality problem throughout the world (Paerl and Huisman, 2008; Pick, 2016). Phytoplankton, as the primary producer, is an essential component of the food web, but excessive growth can alter the ecosystem structure and function (Huisman et al., 2018). Furthermore, toxic substances produced by cyanobacteria can harm aquatic ecosystems and negatively affect the health of both animals and humans (Anderson and Garrison, 1997; Codd et al., 1999; Paerl and Fulton, 2006; Paerl and Paul, 2012; Graham et al., 2020), while complicating and increasing the cost of water treatment (Codd et al., 2005; Srinivasan and Sorial, 2011).

Cyanobacteria occurrence has been studied most often in lentic systems in relation to temperature, light, water column stability, and nutrients (Huisman et al., 2018). Available data suggest that algal community composition responds similarly to nutrient loading, whether in lakes, reservoirs, or rivers (Smith, 2003). In large rivers with adequate nutrients, factors such as flow rate and turbidity determine algal growth (Reynolds and Descy 1996), but river studies are challenging due to complex and variable hydrological conditions (Xia et al., 2020). In a global study, Van Niewenhuyse and Jones (1996) found mean summer chlorophyll-a (Chl-a) in temperate streams bore a curvilinear relationship with total phosphorus (TP), with a secondary influence of catchment size (a surrogate for flow rate and residence time). Graham et al. (2020) reported that nuisance algal blooms occur mainly in eutrophic rivers in North America and that algal toxins in rivers, specifically regulated rivers, are understudied relative to factors that promote HABs in lakes, estuaries, and coastal regions.

* Corresponding author.
E-mail addresses: kimjyo0218@gmail.com (J. Kim), seodi@cnu.ac.kr (D. Seo), JonesJ@missouri.edu (J.R. Jones).

https://doi.org/10.1016/j.ecolmodel.2022.109931
Received 16 August 2021; Received in revised form 9 February 2022; Accepted 1 March 2022
Available online 9 March 2022

Hydraulic structures, such as dams and weirs, are known to adversely affect aquatic ecosystems due to the interference of water movement and disruption of river continuity (Bednarek et al., 2001). The structures reduce horizontal flow velocity and make vertical movement dominant, which favors particulate materials settling to the sediments. Construction of hydraulic structures generally reduces flow rates and increases both residence time and water volume. Seo et al. (2012) reported that increased residence time by hydraulic structures may promote algal blooms even in river reaches with moderate nutrients. Feld et al. (2011) suggested the removal of hydraulic structures can, in time, result in biological restoration, though there may be a temporary negative impact from the disturbance. In contrast, (Cisowska and Hutchins, 2016) estimated that a weir in their study modestly reduced the annual fraction of nitrate load being retained behind the structure but was uncertain how the river would respond to increased nitrogen following weir removal. Cha et al. (2017) suggested that summer cyanobacterial cell counts depended on residence time and water temperature, in rivers regulated by weirs in Korea.

The downstream reach of the Han River traverses the Seoul metropolitan area, where 4 of the nation's largest wastewater treatment plants (WWTPs) discharge effluent. In 1988, an in-stream structure, the Singok Weir, was constructed, which blocked tidal seawater at the mouth of the river to reduce bridge scouring and provide an agricultural water supply. Consequently, HABs have continually occurred and become severe, especially in 2015. Many research shows that the construction of hydrostructures deteriorates water quality, and removal of the weir in the Han River has been considered an option to alleviate nuisance HABs and restore the ecosystem. Kim et al. (2021) reported that the removal of weirs in a regulated river can reduce HABs upstream due to increased flow velocity, but may deteriorate water quality and promote HABs further downstream. The Han River estuary has extremely complicated flow dynamics and water quality kinetics due to a mixture of incoming flows, which includes discharge from Paldang Dam in the headwater, effluents from WWTPs, inflows from urban and nonurban tributaries, and appreciable tidal effects (Kim et al., 2017). The complexity of this system makes it difficult to analyze the effects of weir removal based on insights from previous studies.

The aim of this study was to quantify the effects of hydraulic changes resulting from the removal of the hydraulic structure, the Singok weir, on water quality and HABs occurrences in the Han River estuary. A numerical model was applied to analyze cyanobacteria dynamics in an estuarine environment with complex hydrodynamic and sediment transport conditions due to tidal movements and with complicated biochemical interactions among pollutants.

2. Materials and methods

2.1. Study area and water quality

The Han River is the largest in Korea with a length of 483 km and a basin area of 34,428 km^2. This study includes a 71 km section of the river that passes through Seoul, from the Paldang Dam (Dam) to the Jeonryu water level station (WL7, Fig. 1). Five wastewater treatment plants in Seoul (WWTP1 ~ WWTP4) and in Goyang City (WWTP5) discharge effluents into the study area. Flow and pollutant loadings from major tributaries (Tr1 ~ Tr14) were considered as boundary conditions. Data from 14 water quality monitoring stations (Q1 ~ Q14) and 7 water level monitoring stations (WL1 ~ WL7), managed by the Korean government, were used for model calibration. The Jamsil weir (Weir1) located upstream, which blocks tidal flow from the coast and protects the drinking water source, is 6.4 m high and is located near the Jamsil Bridge (Q6). The Singok weir (Weir2) located downstream, the major weir in this study, is 2.6 m high and is located near the Gimpo Bridge (Q13). The locations of important places and monitoring stations are shown in Fig. 1.

Monthly and yearly discharge from Paldang Dam was analyzed for five years from 2013 to 2017 (www.wamis.go.kr) (Supplemental Figure 1; hereafter S-Fig. 1). Discharge from Paldang Dam was highest in 2013 with an annual average rate of 607 m^3/s and was lowest in 2015 with 177 m^3/s (about 29% of 2013) due to extreme drought.

Water quality changes in the Han River were analyzed over the study period (www.nier.go.kr) (S-Fig. 2). Total organic carbon (TOC), total nitrogen (TN), and TP showed sharp increases between Jamsil Weir (Q6) and Singok Weir (Q13) where WWTPs continuously discharge wastewater in addition to other nonpoint source load inputs from major tributaries in the area. Noteworthy, TN and TP increased more than twice and 10-times, respectively, below Q8 due to the influence of wastewater inputs.

According to stream trophic state criteria for TP (Dodds et al., 1998), the upper reaches (Q1 ~ Q6) can be classified as oligotrophic-mesotrophic, (25 mg/m^3 in S-Fig. 2), while the lower reaches (Q7 ~ Q14) would be considered mesotrophic-eutrophic (75 mg/m^3 in S-Fig. 2). However, TN levels in the study site exceeded mesotrophic-eutrophic criteria, often by several-fold (1.5 mg/L, Dodds et al., 1998), and could not be applied to the Han River. Average Chl-a in all locations was below the mesotrophic-eutrophic criteria (30 mg/m^3, Dodds et al., 1998) though individual values >50 mg/m^3 were common, particularly in the lower reach (Q7 ~ Q14 in S-Fig. 2).

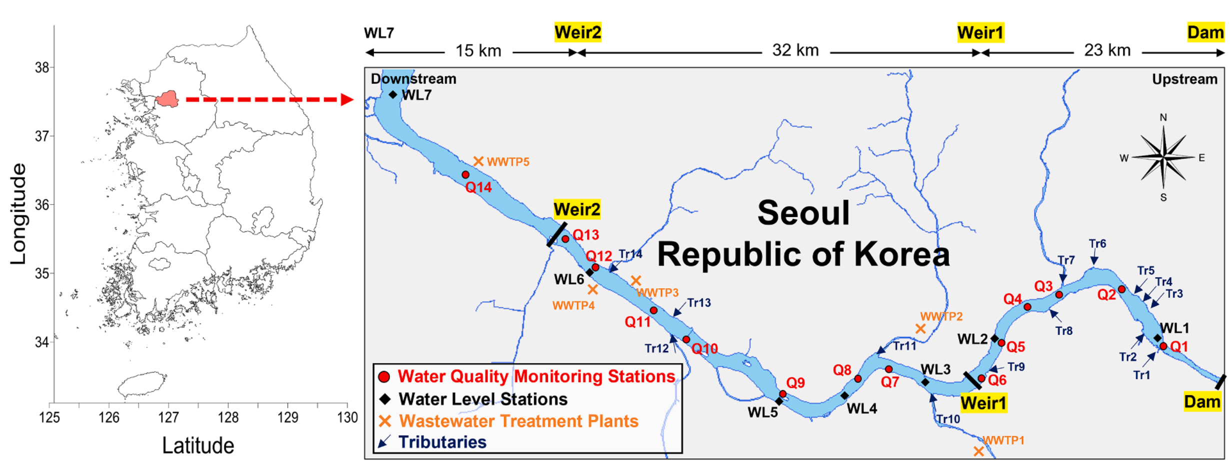

Fig. 1. Map of the lower Han River: Water quality monitoring stations (Q), Water level monitoring stations (WL), Wastewater treatment plant discharge (WWTP), and Major tributaries (Tr).

2.2. Model development and boundary conditions

Water quality models provide a quantitative basis for comprehensive interpretation of complex water quality interactions and thus to develop management alternatives (Thomann and Mueller, 1987; Chapra, 1997; Ambrose et al., 2009). However, in order to reflect and analyze various external and internal interactions, it is important to ensure that the model adequately reflects these conditions. First, the physical transport of the hydraulic structure should be calculated with consideration of a tidal effect. Second, the interaction between water quality variables and algae should be quantitatively linked. Third, sediment transport should be considered to reflect key riverine processes. These characteristics are particularly relevant in downstream regions and estuaries.

The Environmental Fluid Dynamics Code (EFDC) model (Hamrick, 1992) is used to simulate physical, chemical, and microbiological changes in aquatic systems such as rivers, lakes, estuaries, and coastal areas (Park et al., 2005; Li et al., 2011; Wu and Xu, 2011; Tang et al., 2016; Kim et al., 2017, 2021; Bae and Seo, 2018, 2021). In this study, the 8.5 version model of EFDC Explorer Modeling System (www.eemodelingsystem.com) was used. The model included various modules such as hydrodynamics, water temperature, salinity, water quality, and sediment transport. The water quality module is composed of interactions of algae, carbon, nitrogen, phosphorus, silica, oxygen, and fecal coliform bacteria (S-Fig. 3). Algae are further divided into cyanobacteria, diatoms, and green algae. Each phytoplankton group has different growth characteristics such as carbon to Chl-a ratio, optimal growth temperature, and maximum growth rates. Each algal group can be modeled separately, with abundance expressed as Chl-a in mg/m^3. Changes in water quality and cyanobacteria in the lower section of the Han River with the removal of the Singok weir were evaluated using the calibrated model. In this study, macroalgae or rooted phytoplanktons were not simulated.

The computational grid for the EFDC was developed using the curvilinear orthogonal coordinate method and 2029 horizontal cells with the orthogonality deviation of 1.24. Each cell was divided into 5 vertical layers to consider the stratification effect due to salinity from tidal effects. EFDC uses a stretched or sigma grid system for vertical layers and the same number of layers were used for the study area. A three-second time step was used to satisfy the CFL (Courant-Friedrichs-Lewy) condition (Courant et al., 1967), and the CFL number was estimated at <1.0. The average size of the horizontal grid was 130 m x 270 m. Wetting and drying conditions were also considered (S-Fig. 4).

Daily flow data from fourteen tributaries as well as the headwater from Paldang Dam, five wastewater treatment plants, and twelve water intake systems were used as flow boundary conditions. Open boundary conditions were established to reflect the tidal movement along the west coast. To address water level fluctuations of around 3 m, hourly data were applied (S-Fig. 5).

Water quality data from the tributaries were available from irregular intervals, ranging between 1 ~ 5 times a month. All data were linearly interpolated to make daily data for boundary conditions values and applied in the EFDC model. Based on the cell count data measured by Seoul City (Supplemental Table 1, hereafter S-Table 1), algae were divided into cyanobacteria, diatoms, and green algae. The time series of the water quality and salinity for the estuary boundary condition were considered using data from Q14, including TSS values used in the sediment transport model. Salinity values were not available for the study area and were derived from water temperature and conductivity (Fofonoff and Millard, 1983). In the sediment transport model, data were subdivided into cohesive and non-cohesive sediment categories according to Zhang et al. (2011), and the settling velocity of cohesive sediment was estimated using data from Kim et al. (2015). All the necessary field data for simulation was obtained from the Korean governmental database management systems. The Water Information System (water.neir.go.kr) was used for water quality data, and the Water Resources Management Information System (wamis.go.kr) was used for flow rates and water level data. Data on weather and wind conditions were obtained from the Korea Meteorological Administration (data.kma.go.kr).

2.3. Calibration and scenario development

Calibrations of the hydrodynamics and water quality model were performed using data from 2013 to 2017 (S-Fig. 6 and S-Table 2). Water level calibration was based on data from six water level monitoring stations (WL1 ~ WL6). For calibration of water temperature and water quality, data from fourteen water quality monitoring stations (Q1 ~ Q14) were used. Water quality variables were TOC, TN, TP, Chl-a, dissolved oxygen (DO), ammonia nitrogen (NH3), nitrate nitrogen (NO3), dissolved inorganic phosphorus (DIP or total phosphate), and total suspended solids (TSS). Accuracies of calibration results were calculated using Root Mean Square Error (RMSE) and index of agreement (IA, Willmott, 1981) (S-Table 2). RMSE is the size of a typical error. IA is the ratio between the mean square error and potential error (Willmott, 1984) and can be used as a substitute for the coefficient of determination (Legates and McCabe Jr, 1999). RMSE ranges from 0 (the ideal value) to ∞. IA is calculated from 0 to 1 (the ideal value). The parameters were initially chosen from previous research results (Bowie et al., 1985; Cole and Wells, 2006; Shin et al., 2008) and adjusted further to improve calibration accuracy (S-Table 3). The calibration of this study was based on previous EFDC applications for the same study site by Kim et al. (2017). This analysis used improved grid resolution and field data over a longer period with consideration of sediment transport. Total chlorophyll-a is the summation of all simulated algal groups, and this was used for Chl-a calibration because the data are available in the national database system in Korea (www.nier.go.kr).

Changes in the hydraulic dynamics, water quality, and HAB occurrences in the lower part of the Han River due to the Singok weir were evaluated with the model. The scenario "With" indicates when the Singok weir exists which is the same as the current conditions. The scenario "Without" predicts conditions if the Singok weir was removed.

3. Results and discussion

3.1. Effects of annual water quality changes due to weir removal

To analyze the effect of the weir removal, the analysis was focused on the 30 km reach between Jamsil weir and Singok weir (hereafter Weir), though model simulation was performed for the entire 71 km river reach. Also, the study reach was subdivided into three regions for detailed analysis; the upper region (Q7), middle region (Q10), and lower region (Q12); located 24 km, 12 km, and 2 km upstream from Weir, respectively (S-Fig. 4). Volume-weighted averages were used from 20 cells around each station to strengthen the representation of the area to avoid a possible bias of a value from a particular cell. For the weighted averaged values, simulated values for the "Without" scenario were compared with the "With" scenario at the upper, middle, and lower regions, respectively.

Weir removal would reduce water levels by approximately 14%, which may reduce water volume, given that the river cross-section is trapezoidal (Table 1). Weir removal will restore the influence of tidal flow upstream. The extent of tidal influence can be assessed by periodic water level fluctuations. After removal of the weir, water level fluctuation became greater up to the upper region (Q7) due to the increased tidal effect (S-Fig. 7).

Annual average water quality concentrations in the study area would largely be controlled by dilution from the mixture of headwater, tributary flows, WWTP discharges, and tidal flow along with kinetic transformations. As water levels declined due to the weir removal, concentrations of water quality constituents increased with reduced water volume and unchanged waste loading introduced to the river. TN and TP increased 1 ~ 5% and 2 ~ 11%, respectively. NH3+NO3 (or DIN,

Table 1
Average water level changes due to the weir removal in the study area.

Variable	Year	Q7 (Upper)			Q10 (Middle)			Q12 (Lower)		
		With	Without	%	With	Without	%	With	Without	%
Water Level [EL.m]	2013	3.35	3.07	91.9	3.23	2.94	91.0	3.18	2.89	90.8
	2014	2.84	2.44	86.1	2.80	2.39	85.3	2.79	2.37	85.1
	2015	2.75	2.27	82.8	2.73	2.25	82.4	2.72	2.24	82.4
	2016	2.94	2.55	86.9	2.89	2.49	86.3	2.87	2.48	86.2
	2017	3.07	2.66	86.8	2.99	2.57	86.1	2.96	2.54	85.9
	Avg.	2.99	2.60	86.9	2.93	2.53	86.3	2.90	2.50	86.2

dissolved inorganic nitrogen) and DIP also increased up to 5.2% and 37%, respectively (Fig. 2 and S-Table 4). Increasing rates of TSS were much greater at Q12 (Lower) (126 ~ 214%) compared to at Q7 (Upper) (107 ~ 132%) due to increased sediment resuspension and transport by tidal action following the weir removal (Van Rijn, 1993). Temperature decreased modestly (0.01 ~ 0.06 °C or 0.1 ~ 1.1%) in the upper region and increased in the middle and lower region (0.04 ~ 1.31 °C or 0.3 ~ 2.6%). Changes in average salinity concentrations increased by 0.001 ~ 0.002 psu at Q12 and were considered negligible throughout the study area (S-Table 4).

3.2. Effect of water velocity or hydraulic residence time changes

Annual average water velocity in the upper region increased by about 0 ~ 0.42 km/day (This velocity unit was used rather than m/*sec* to convey flow in the reach) due to the weir removal (Fig. 3 and S-Table 5). However, water velocity decreased by 0.04 ~ 0.53 km/day in the middle region and 0.14 ~ 1.01 km/day in the lower region. Therefore, hydraulic residence time would decrease at the upper region (Q7) and increase in the middle region (Q10) and the lower region (Q12), which would affect the available time for algal growth in the respective region. Annual average water velocity was the lowest at Q10 (middle), the deepest part in the study region, due to its large cross-sectional area. These conditions may make Q10 a region of more favorable for algal growth and also affect the greatest algal biomass in the lower region (Q12) each year. Reynolds and Descy (1996) stated that in-channel phytoplankton growth is strongly influenced by characteristics of the hydrologic stage.

However, summer average velocity (July-September) showed mixed results in the middle and lower regions. Except for 2014 and 2015, summer average velocity increased in the middle and lower regions after weir removal (Fig. 3 and S-Table 5). In general, the summer Monsoon in Korea results in higher flow rates during the flood season (Jones et al., 2009). However, summer discharges in 2014 and 2015 were reduced due to severe drought in those years (S-Fig. 1). Summer velocity in the middle and lower regions decreased after the weir removal in those two years. This finding indicates that though the weir removal can increase water velocity during the flood season, but would decrease average water velocity in drought.

3.3. Effect of phytoplankton and cyanobacteria growth

Annual average phytoplankton (as chlorophyll-a) decreased 1 ~ 7% or 1 ~ 3 mg/m^3 in all cases due to the weir removal except in the lower region in 2015, where it showed a modest increase of 0.21 mg/m^3 or 0.6% (S-Table 6). Annual average cyanobacteria decreased in the upper region in all years but showed varied results in the middle and lower regions. During 2015 ~ 2016, average cyanobacteria biomass as chlorophyll-a increased 3 ~ 4% or 0.23 ~ 0.37 mg/m^3 at Q12.

In summer (July-September) when excessive cyanobacteria biomass can occur, after the weir removal, average cyanobacteria decreased by 0.6 ~ 5.4% in the upper region but increased by 0.2 ~ 15.3% in the lower region (Table 2). In particular, in 2015, the cyanobacteria biomass in the lower region increased by 4.8 mg/m^3 (15.3%). However, the weir removal did not noticeably change cyanobacteria biomass except in summer 2015 in the middle and lower regions.

After the weir removal, simulations of the spatial distribution of cyanobacteria in late-August 2015 showed greater uniformity in biomass within the water column, especially in the deep area in the middle region near Q10 (Fig. 4-(A) and 4-(B)). During summer 2015, cyanobacteria distribution would become more widely dispersed both horizontally and vertically in response to greater mixing due to increased tidal movement following the weir removal.

3.4. Changes in factors limiting algal growth following weir removal

Phosphorus promotes eutrophication and algal growth in freshwater (Correll, 1998), however other factors such as physical conditions can be influential. Fig. 5 shows a curvilinear TP-Chl-a relation in temperate streams (Van Nieuwenhuyse and Jones, 1996) with summer field data

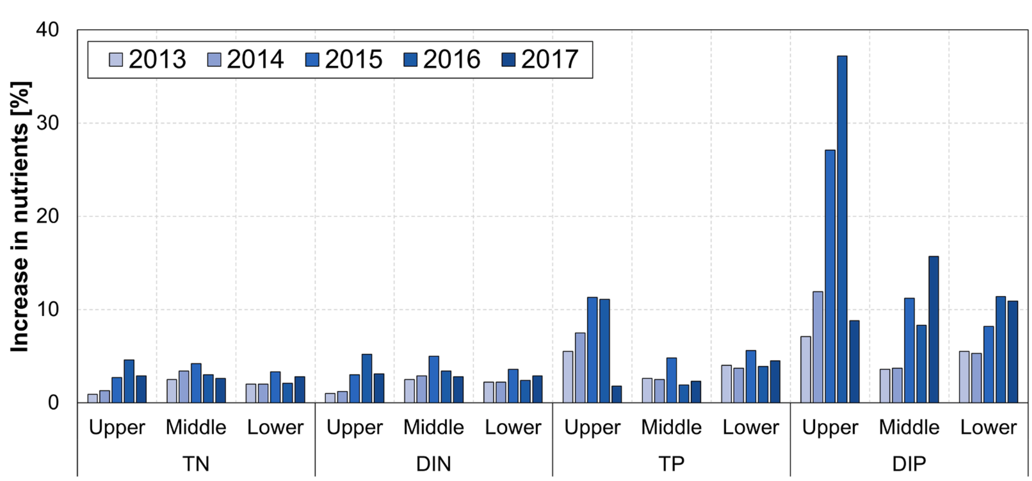

Fig. 2. Annual average changes in nutrient concentrations due to the weir removal.

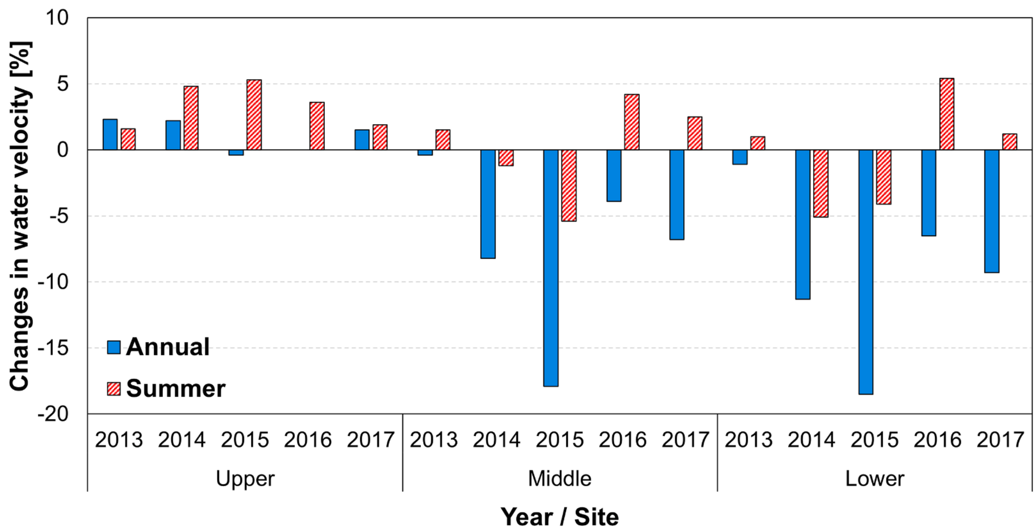

Fig. 3. Average changes in water velocity due to the weir removal.

Table 2
Summer average cyanobacteria changes due to the weir removal.

Variable	Year	Q7 (Upper)			Q10 (Middle)			Q12 (Lower)		
		With	Without	%	With	Without	%	With	Without	%
Chl-a [mg/m^3]	2013	0.57	0.56	99.4	0.89	0.88	99.8	1.11	1.13	101.3
	2014	2.30	2.25	97.7	3.99	3.93	98.6	4.90	4.84	98.7
	2015	14.37	13.60	94.6	36.99	38.48	104.0	31.43	36.24	115.3
	2016	10.28	10.16	98.8	10.69	10.97	102.7	12.50	13.24	105.9
	2017	4.92	4.88	99.1	5.77	5.76	99.8	5.94	5.95	100.2

from the study sites superimposed on the relationship. Data from Q1 ~ Q6 (Open circles) represent upstream conditions, where TP and Chl-a averaged 40 mg/m^3 and 13.2 mg/m^3, respectively. Data from Q7 ~ Q14 (Black circles) represent conditions in the reach polluted by WWTP discharge, where TP and Chl-a averaged 162 mg/m^3 and 19.5 mg/m^3, respectively. Observed values in the upper reach averaged 27% greater than the temperate pattern, while values from the nutrient-rich lower reach were 7% below, with extreme scatter in the data. This comparison illustrates that factors other than TP can influence algal biomass in the Han River.

Algal growth rates depend on nutrient availability, water temperature, light intensity, and salinity ((Cerco and Cole, 1993); Di Toro et al., 1971) (Supplemental Equation 1, hereafter S-Eq. 1). Fig. 6 and S-Table 7 summarize the changes in percentage for the growth limiting factors of summer cyanobacteria following weir removal. Positive values indicate more favorable growth conditions.

Nutrient limitation of algal growth was estimated using Liebig's "law of the minimum" principle (Odum and Barrett, 1971, S-Eq. 2) in the model. Nitrogen limitation for cyanobacterial growth was not changed in most stations. In the study area, the smallest TN/TP ratio and DIN/-DIP ratio were calculated as 23.3 and 32.8, respectively (S-Figure 8). These values indicate nitrogen was not a limiting factor in this system and would not likely affect changes in algal growth rate in the study site for the weir removal (Forsberg and Ryding, 1980; Thomann and Mueller, 1987). In contrast, phosphorus limitation was indicated, especially in 2015 and 2016. Percent changes in the summer nutrient limitation based on phosphorus were positive in the upper (+5.26%) and middle (+1.09%) regions and negative for the lower (−0.29%) region in 2015. The upper and middle regions showed an increase in nutrient concentration due to decreased water volume, as discussed previously. Decreased phosphorus limitation in the lower region indicated the increased consumption of DIP due to increased cyanobacteria growth in the middle region (Q10). Similar findings were reported by Kim et al. (2021) during their algal bloom analysis in the Geum River, Korea.

Light limitation of algal growth was calculated using depth-averaged Steele's equation (Steele, 1965, S-Eq. 3 ~ 6). The extinction coefficient was calculated as functions of Chl-a, organic matter, and suspended solids (Di Toro, 1978) in the EFDC model. Increased TSS concentration due to the tidal effect by weir removal would increase light extinction and thus decrease light penetration. While lower water levels resulting from weir removal would increase the average available light for algal growth. Therefore, the overall light limitation would be a combination of above the two effects. Fig. 6 shows the light limiting factor would decrease during summer, especially in the middle and lower regions. Changes in the light growth limitation factor in the upper region were smaller than the other regions because TSS concentrations increased due to tidal sediment were much less (<1.6 mg/L) as shown in S-Table 4.

Temperature limitation for algal growth was calculated using the Gaussian probability curve ((Cerco and Cole, 1993), S-Eq. 7). Annual average temperature becomes 0.04 ~ 0.41 °C higher in the middle and lower regions while it becomes 0.01 ~ 0.16 °C lower in the upper region. These changes in summer temperature growth limiting factor, however, seem negligible as shown in Fig. 6 through the middle region in 2015 increased slightly (0.005 ~ 0.010) following the weir removal.

Salinity limitation for cyanobacterial growth was calculated using S-Eq. 8 (Cerco and Cole, 1993). Because salinity concentrations were close to 0 psu in both scenarios, salinity limitation on cyanobacterial growth was considered negligible.

Table 3 summarizes the changes in the total growth limiting factors of cyanobacteria in summer calculated by the multiplication of nutrient, light, temperature, and salinity limiting factors. In general, growth limiting factors tended to increase with the weir removal. This result suggests that the weir removal can enhance algal growth potential in the Han River, however, differences in the net growth limitation factors were in the range of 0.001 and 0.031, which seemed unimportant. It is notable that the summer growth limitation of 2015 in the lower region

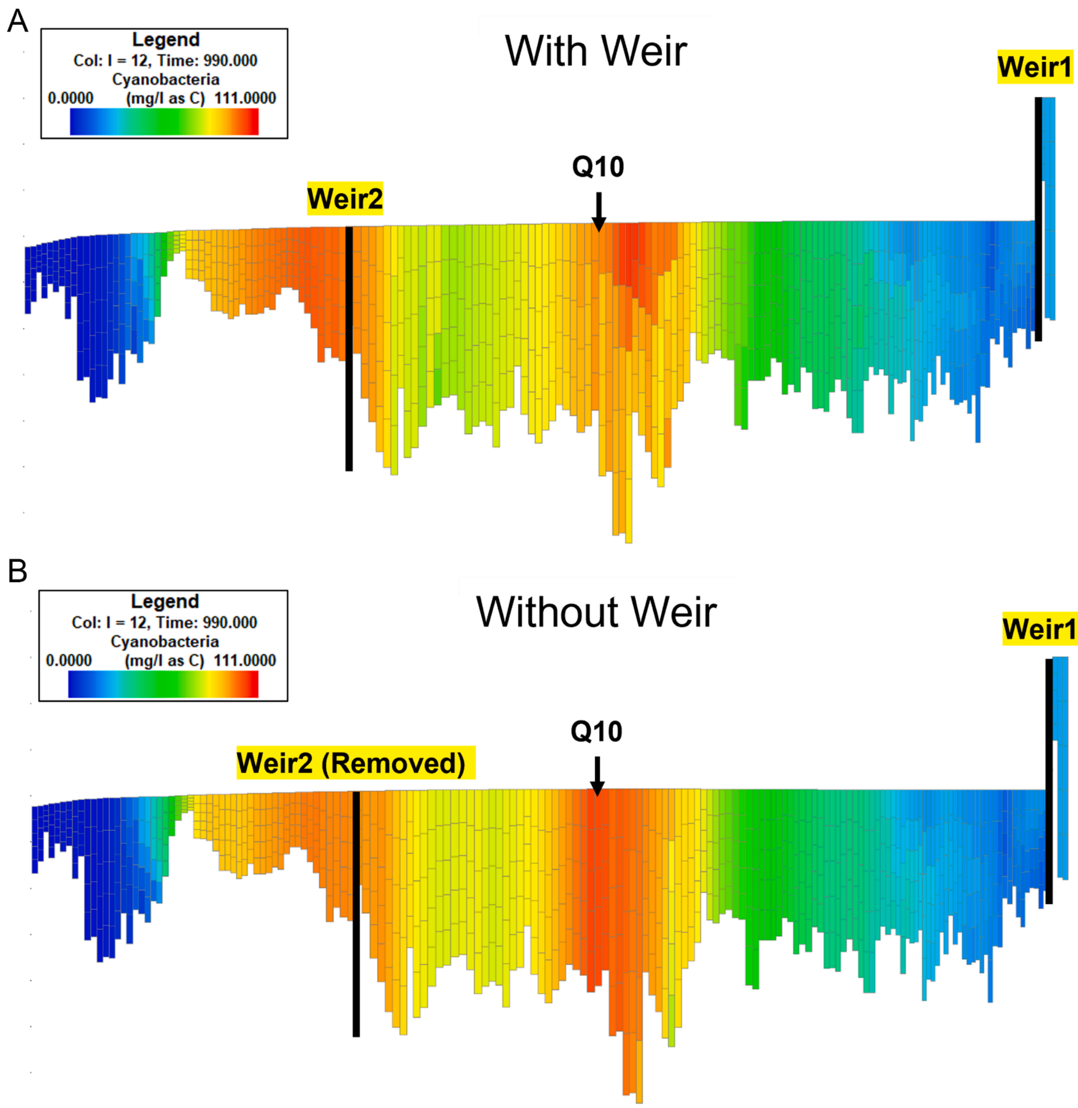

Fig. 4. Cyanobacteria distribution on August 31 in 2015 (990 day). (A): With Weir and (B): Without Weir.

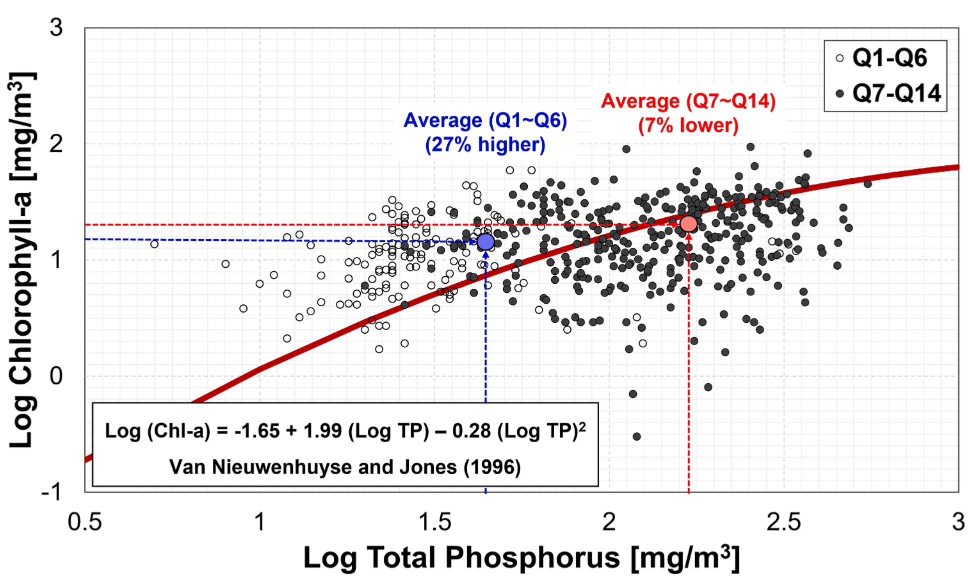

Fig. 5. Summer TP-Chl-a relation in temperate streams (Van Nieuwenhuyse and Jones, 1996) and field data from study sites in the Han River.

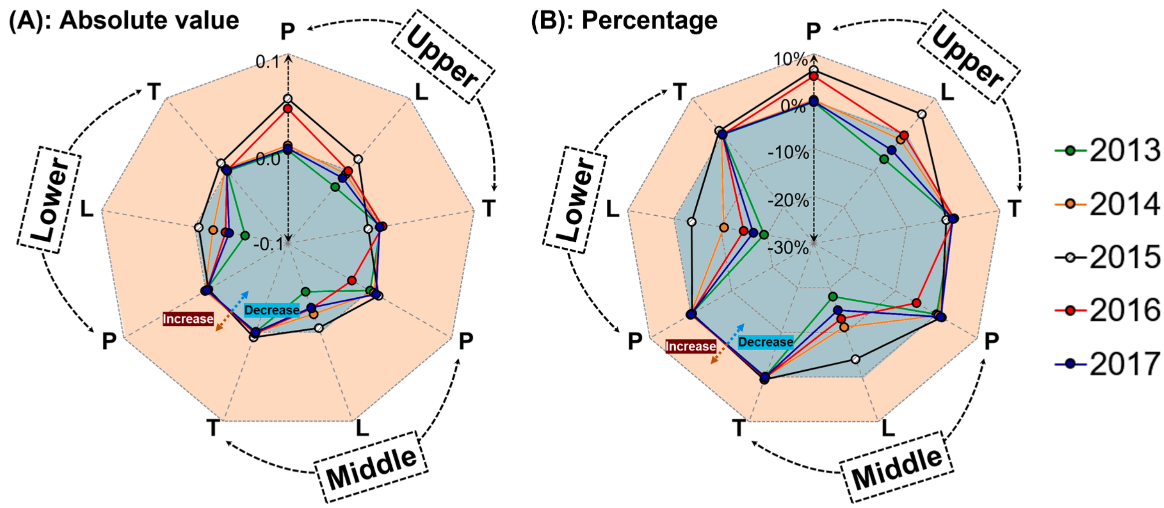

Fig. 6. Changes in the growth limiting factor for cyanobacteria due to weir removal during the summer (The orange and blue areas indicate positive and negative, respectively; P: Phosphorus, L: Light, T: Temperature).

Table 3
Net growth limiting factor of cyanobacteria due to the weir removal during the summer.

Year	Q7 (Upper)			Q10 (Middle)			Q12 (Lower)		
	With	Without	%	With	Without	%	With	Without	%
2013	0.182	0.181	99.7	0.144	0.144	100.0	0.156	0.152	97.4
2014	0.242	0.266	109.7	0.134	0.145	108.2	0.135	0.151	112.0
2015	0.212	0.243	114.4	0.074	0.090	120.9	0.101	0.104	103.2
2016	0.187	0.209	111.7	0.052	0.052	100.9	0.157	0.158	100.7
2017	0.123	0.126	102.4	0.072	0.075	103.6	0.125	0.121	96.4

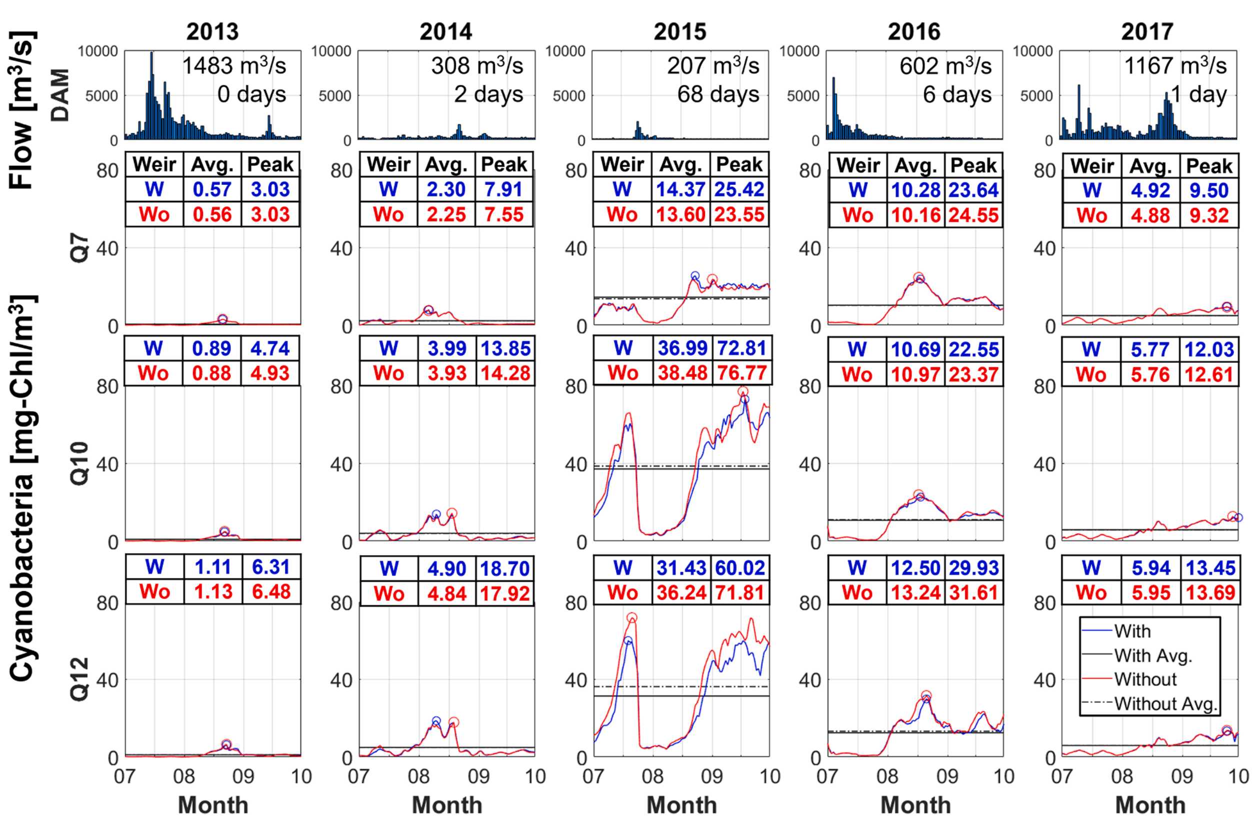

Fig. 7. Headwater discharges (with summer average flow rate and days less than 150 m^3/s between July–Sept) and cyanobacteria dynamics (values in the box represent average and peak values of cyanobacteria during July-Sept with (W) and without (Wo) the weir).

(Q12) was around 0.1 and this is the lowest in the study period. Light availability seems to be the major factor during the low-flow year, as shown in Fig. 6.

3.5. Headwater conditions following weir removal

Fig. 7 shows Paldang dam discharge rates and simulated cyanobacteria biomass changes in the summer with and without the weir. There were no meaningful changes in cyanobacteria biomass due to the weir removal except during summer 2015, which is consistent with Table 2. In 2015, the summer average and peak cyanobacteria in the lower (Q12) region increased by 15% or 4.8 mg/m^3 and 20% or 11.8 mg/m^3 in response to the weir removal. Noteworthy, summer average cyanobacteria was highest in the middle (Q10) region only in 2015 while both average and peak values were highest in the lower (Q12) region in other years. This may be caused by reduced water velocity in the middle region (Q10) following the weir removal as shown in Fig. 3. In 2015, with the weir removal, the summer average water velocity in the middle (Q10) region was estimated to be 3.2 km/day, which indicates that it would take about 3 days to travel 10 km from Q10 to Q12. Using this calculation protocol, summer travel time between the middle and lower regions (Q10 ~ Q12) in 2014 and 2016 was estimated at approximately 2 days and 1 day, respectively. Algal growth rate is an exponential function with time (Di Toro et al., 1971), so longer residence time would allow exponentially greater cyanobacterial biomass. Excessive growth of cyanobacteria would consume DIP in the middle (Q10) region, which would reduce nutrient availability in the lower (Q12) region. Kim et al. (2021) reported that excessive growth of phytoplankton upstream can result in depletion of DIP and reduced algal growth downstream in a large regulated river.

In contrast, in 2013 and in 2017, when the average flows were greater than other years, differences in summer cyanobacteria biomass due to the weir removal were modest with the maximum difference of 0.58 mg/m^3. Therefore, it can be concluded that the weir removal did not show an appreciable change in summer cyanobacteria dynamics in non-drought years. In 2014 and 2016, which are relatively low-flow years, the summer average and peak cyanobacteria increments were greater than in 2013 and 2017.

Fig. 7 also shows that cyanobacteria dynamics exhibit exactly the opposite pattern with headwater discharge. When there was increased flow, cyanobacteria biomass declined rapidly and when the flow was reduced, cyanobacteria biomass increased, which emphasizes the importance of hydraulics on cyanobacterial growth. This effect was especially pronounced in summer 2015. Moreover, the 2015 drought was a historically significant impact of the El Niño–Southern Oscillation (ENSO; Philander, 1983), which indicates severe cyanobacterial growth would intensify whenever similar ENSO conditions occur (Li et al., 2020; Liu et al., 2017; Zhang et al., 2018). In Fig. 7, the summer average flow rate and the number of days when dam discharge was less than 150 m^3/s (chosen by visual inspection) during the summer were denoted. When flow rates were continuously lower than this value, cyanobacteria biomass continuously increased, but with increased discharge cyanobacteria biomass dropped immediately.

According to Table 3 and Fig. 7, these analyses emphasize the importance of hydraulics, or residence time, as the key factor controlling algal blooms in rivers with sufficient nutrients, as reported by other researchers (Reynolds and Descy, 1996; Jones and Elliott, 2007; Li et al., 2011; Seo et al., 2012; Graham et al., 2020, (Xia et al., 2020). In conclusion, if the algal growth potential is high but sufficient residence time is inadequate, algal growth is limited. In contrast, if the growth potential of algae is low but sufficient residence time is adequate, the algae proliferate.

4. Conclusions

This study evaluated changes in water quality and cyanobacteria biovolume in the Han River estuary with the removal of Singok Weir. The 3-D hydrodynamics, water quality, and sediment transport models in EFDC were applied in combination to account for complicated water movement, water quality kinetics, and algal growth responses. Responses in water quality, total phytoplankton, and cyanobacteria biovolumes are different spatially and temporally. The response analyses were performed intensively for three distinct locations, Q7 (upstream), Q10 (middle stream), and Q12 (downstream) each are 2 km, 12 km, and 24 km above Singok weir, respectively.

Annual average nutrients and organic concentrations due to the weir removal were controlled by dilution from the headwater, tributary flows, WWTPs, and tidal flows each year. As the annual average water level declined by 9.2 ~ 17.5% due to the weir removal, concentrations of water quality constituents increased given the same waste load to the study site. Annual average TN and TP increased by 1 ~ 5% (0. 1 ~ 0.24 mg/L), 2 ~ 11% (0.001 ~ 0.015 mg/L), respectively. Annual average TSS increased 8.1 ~ 114% (1 ~ 41 mg/L) due to increased sediment load from the tidal inflow. Annual average phytoplankton decreased by 1 ~ 7% (1 ~ 3 mg Chl-a/m^3). Annual average cyanobacteria biovolume decreased only in the upstream area while it showed mixed results in the other regions.

In summer (July-September), average cyanobacteria decreased by up to 5.4% (0.8 mg/m^3) in the upper region but increased by up to 15.3% (4.8 mg/m^3) in the lower region due to the weir removal. In particular, in the driest year, 2015, peak cyanobacteria biomass in the lower (Q12) region increased by 20% (11.8 mg/m^3). The corresponding changes in hydraulic residence time seem to be the principal factor determining biomass. However, summer average cyanobacteria differences in most years were less than 1.0 mg Chl-a/m^3 except the extremely dry year, 2015. During the summer, cyanobacteria distribution would become more widely dispersed, both horizontally and vertically in response to increased tidal movement. This result emphasizes the importance of seasonal and hydrodynamic assessment when analyzing cyanobacteria in response to external changes, which can be masked in annual average values by numerous factors.

Factors for algal growth increased during summer suggesting that the weir removal can enhance seasonal algal growth potential in the Han River. The effect of the weir removal tended to be greater in the upper reach during low flow and light limitation seemed to be the dominant factor. However, differences in the increment in net growth limitation factors were modest (<0.031).

Noteworthy, the role of hydrology stood out as the major factor determining algal growth, with greater relative importance than nutrients, light, and temperature. The major factor determining factor for harmful algal growth in the lower area in 2015 was residence time, which was affected by the discharge of headwater Paldang Dam. When flow rates were continuously lower than 150 m^3/s, cyanobacteria biomass increased, but with increased discharge, cyanobacteria biomass dropped immediately. In conclusion, when the algal growth potential is high, as in the Han River, hydrology determines biomass.

CRediT authorship contribution statement

Jaeyoung Kim: Conceptualization, Methodology, Software, Formal analysis, Validation, Visualization, Writing – original draft. **Dongil Seo:** Conceptualization, Methodology, Supervision, Resources, Formal analysis, Validation, Visualization, Writing – review & editing. **John R. Jones:** Formal analysis, Validation, Writing – review & editing.

Declaration of Competing Interest

The authors declare that they have no known competing financial interests or personal relationships that could have appeared to influence the work reported in this paper.

Supplementary materials

Supplementary material associated with this article can be found, in the online version, at doi:10.1016/j.ecolmodel.2022.109931.

References

Ambrose Jr., R.B., Wool, T.A., Barnwell Jr., T.O., 2009. Development of water quality modeling in the United States. Environ. Eng. Res 14, 200–210. https://doi.org/10.4491/eer.2009.14.4.200.

The ecology and oceanography of harmful algal blooms. In: Anderson, D.M., Garrison, D. J. (Eds.), The ecology and oceanography of harmful algal blooms. Am. Soc. Limnol. Oceanography 42, 1007–1009.

Bae, S., Seo, D., 2018. Analysis and modeling of algal blooms in the Nakdong River, Korea. Ecol. Modell. 372, 53–63. https://doi.org/10.1016/j.ecolmodel.2018.01.019.

Bae, S., Seo, D., 2021. Changes in algal bloom dynamics in a regulated large river in response to eutrophic status. Ecol. Modell 454, 119590. https://doi.org/10.1016/j.ecolmodel.2021.109590.

Bednarek, A.T., 2001. Undamming rivers: a review of the ecological impacts of dam removal. Environ Manage 27, 803–814. https://doi.org/10.1007/s002670010189.

Bowie, G.L., Mills, W.B., Porcella, D.B., Campbell, C.C., Pagenkopf, J.R., Rupp, G.L., Johnson, K.M., Chan, R.W.H., Gherini, S.A., Chamberlin, C.E., 1985. Rates, Constants and Kinetics Formulations in Surface Water Quality Modeling. Environment Research Laboratory, Environmental Protection Authority. Second edEPA/600/385/040.

Cerco, C.F., Cole, T., 1993. Three-dimensional eutrophication model of Chesapeake Bay. J. Environ. Eng. 119 (6), 1006–1025.

Cha, Y., Cho, K.H., Lee, H., Kang, T., Kim, J.H., 2017. The relative importance of water temperature and residence time in predicting cyanobacteria abundance in regulated rivers. Water Res. 124, 11–19. https://doi.org/10.1016/j.watres.2017.07.040.

Chapra, S.C., 1997. Surface Water-quality Modeling. McGraw-Hill Series in Water Resources and Environmental Engineering Index. McGraw-Hill, New York.

Cisowska, I., Hutchins, M.G., 2016. The effect of weirs on nutrient concentrations. Sci. Total Environ 542, 997–1003. https://doi.org/10.1016/j.scitotenv.2015.10.064.

Codd, G.A., BELL, S.G., Kaya, K., WARD, C.J., BEATTIE, K.A., METCALF, J.S., 1999. Cyanobacterial toxins, exposure routes and human health. Eur. J. Phycol. 34, 405–415. https://doi.org/10.1017/s0967026299002255.

Codd, G.A., Morrison, L.F., Metcalf, J.S., 2005. Cyanobacterial toxins: risk management for health protection. Toxicol. Appl. Pharmacol. 203, 264–272. https://doi.org/10.1016/j.taap.2004.02.016.

Cole, T.M., Wells, S.A., 2006. CE-QUAL-W2: A Two-dimensional, Laterally Averaged, Hydrodynamic and Water Quality Model, Version 3.5. Instruction Report EL-06-1. US Army Engineering and Research Development Center, Vicksburg, MS.

Correll, D.L., 1998. The role of phosphorus in the eutrophication of receiving waters: a review. J. Environ. Qual. 27 (2), 261–266. https://doi.org/10.2134/jeq1998.00472425002700020004x.

Courant, R., Friedrichs, K., Lewy, H., 1967. On the partial difference equations of mathematical physics. IBM J. Res. Dev 11, 215–234. https://doi.org/10.1147/rd.112.0215.

Di Toro, D.M., O'Connor, D.J., Thomann, R.V., 1971. A dynamic model of the phytoplankton population in the Sacramento—San Joaquin Delta. Adv. Chem 106, 131–180. https://doi.org/10.1021/ba-1971-0106.ch005.

Di Toro, D.M., 1978. Optics of turbid estuarine waters: approximations and applications. Water Res. 12, 1059–1068. https://doi.org/10.1016/0043-1354(78)90051-9.

Dodds, W.K., Jones, J.R., Welch, E.B., 1998. Suggested classification of stream trophic state: distributions of temperate stream types by chlorophyll, total nitrogen, and phosphorus. Water Res. 32 (5), 1455–1462.

Feld, C.K., Birk, S., Bradley, D.C., Hering, D., Kail, J., Marzin, A., Melcher, A., Nemitz, D., Pedersen, M.L., Pletterbauer, F., Pont, D., Verdonschot, P.F.M., Friberg, N., 2011. Chapter three — from natural to degraded rivers and back again: a test of restoration ecology theory and practice. Adv. Ecol. Res 44, 119–209. https://doi.org/10.1016/B978-0-12-374794-5.00003-1.

Fofonoff, N.P., Millard, R.C., 1983. Algorithms for computation of fundamental properties of seawater. UNESCO technical paper in marine science 44.

Forsberg, C., Ryding, S.O., 1980. Eutrophication parameters and trophic state indices in 30 Swedish waste-receiving lakes. Arch. Hydrobiol. 89, 189–207.

Graham, J.L., Dubrovsky, N.M., Foster, G.M., King, L.R., Loftin, K.A., Rosen, B.H., Stelzer, E.A., 2020. Cyanotoxin occurrence in large rivers of the United States. Inland Waters 10 (1), 109–117. https://doi.org/10.1080/20442041.2019.1700749.

Hamrick, J.M., 1992. A three-dimensional environmental fluid dynamics computer ode: theoretical and computational aspects. Special Report. Virginia institute of Marine Science, College of William and Mary, Gloucester Point, VA, p. 317. https://doi.org/10.21220/V5TT6C.

Huisman, J., Codd, G.A., Paerl, H.W., Ibelings, B.W., Verspagen, J.M.H., Visser, P.M., 2018. Cyanobacterial blooms. Nat. Rev 16, 471–483.

Jones, J.R., McEachern, P., Seo, D., 2009. Empirical evidence of monsoon influences on Asian Lakes. Aquat. Ecosyst. Health Manag. 12 (2), 129–137. https://doi.org/10.1080/14634980902907342.

Jones, I.D., Elliott, J.A., 2007. Modelling the effects of changing retention time on abundance and composition of phytoplankton species in a small lake. Freshw. Biol. 52, 988–997. https://doi.org/10.1111/j.1365-2427.2007.01746.x.

Kim, D.H., Seo, Y.D., Hwang, K.N., 2015. Seasonal variation of settling velocities of cohesive sediments from Han estuary. J. Korean Soc. Coastal Disaster Prevent 2, 99–106.

Kim, J., Lee, D., Seo, D., 2017. Algal bloom prediction of the lower Han River, Korea using the EFDC hydrodynamic and water quality model. Ecol. Modell 366, 27–36. https://doi.org/10.1016/j.ecolmodel.2017.10.015.

Kim, J., Jones, J.R., Seo, D., 2021. Factors affecting harmful algal bloom occurrence in a river with regulated hydrology. J. Hydrol 33, 100769. https://doi.org/10.1016/j.ejrh.2020.100769.

Legates, D.R., McCabe Jr., G.J., 1999. Evaluating the use of "goodness-of-fit" measures in hydrologic and hydroclimatic model validation. Water Resour. Res. 35 (1), 233–241. https://doi.org/10.1029/1998WR900018.

Li, J., Huang, J.-.G., Tardif, J.C., Liang, H., Jiang, S., Zhu, H., Zhou, P., 2020. Spatially heterogeneous responses of tree radial growth to recent El Niño southern-oscillation variability across East Asia subtropical forests. Agric. For. Meteorol. 287, 107939 https://doi.org/10.1016/j.agrformet.2020.107939.

Li, Y., Acharya, K., Yu, Z., 2011. Modeling impacts of Yangtze River water transfer on water ages in Lake Taihu, China. Ecol. Eng. 37, 325–334. https://doi.org/10.1016/j.ecoleng.2010.11.024.

Liu, J., Bowman, K.W., Schimel, D.S., Parazoo, N.C., Jiang, Z., Lee, M., Bloom, A.A., Wunch, D., Frankenberg, C., Sun, Y., 2017. Contrasting carbon cycle responses of the tropical continents to the 2015–2016 El Niño. Science 358 (6360), eaam5690. https://doi.org/10.1126/science.aam5690.

Odum, E.P., Barrett, G.W., 1971. Fundamentals of Ecology. W.B. Saunders Co., Philadelphia, PA.

Paerl, H.W., Fulton, R.S., 2006. Ecology of harmful cyanobacteria. In: Graneli, E., Turner, J. (Eds.), In Ecology of Harmful Marine Algae. Springer-Verlag, Berlin, Germany, pp. 95–107.

Paerl, H.W., Huisman, J., 2008. Blooms like it hot. Science 320, 57–58. https://doi.org/10.1126/science.1155398.

Paerl, H.W., Paul, V.J., 2012. Climate change: links to global expansion of harmful cyanobacteria. Water Res. 46, 1349–1363. https://doi.org/10.1016/j.watres.2011.08.002.

Park, K., Jung, H.S., Kim, H.S., Ahn, S.M., 2005. Three-dimensional hydrodynamic-eutrophication model (HEM-3D): application to Kwang-YangBay, Korea. Maritime Environ. Res. 60, 171–193. https://doi.org/10.1016/j.marenvres.2004.10.003.

Philander, S., 1983. El Niño Southern Oscillation phenomena. Nature 302, 295–301. https://doi.org/10.1038/302295a0.

Pick, F.R., 2016. Blooming algae: a Canadian perspective on the rise of toxic cyanobacteria. Can. J. Fish. Aquat. Sci 73, 1149–1158. https://doi.org/10.1139/cjfas-2015-0470.

Reynolds, C.S., Descy, J.P., 1996. The production, biomass and structure of phytoplankton in large rivers. Large Rivers 10, 161–187. https://doi.org/10.1127/lr/10/1996/161.

Seo, D., Kim, M., Ahn, J.H., 2012. Prediction of chlorophyll-a changes due to weir constructions in the Nakdong River using EFDC-WASP modelling. Environ. Eng. Res 17, 95–102. https://doi.org/10.4491/eer.2012.17.2.095.

Shin, C.M., Na, E.H., Park, J.D., Park, J.H., Lee, S.W., Jeong, J.H., Rhew, D.H., Jeong, D. I., 2008. Application of Parameters and Coefficients of River Water Quality Model For TMDL Plan in Korea. National Institute of Environmental Research, NIERNO, 2008-29-979.

Smith, V.H., 2003. Eutrophication of freshwater and coastal marine ecosystems a global problem. Environmental Science and Pollution Research 10 (2), 126–139. https://doi.org/10.1065/espr2002.12.142.

Srinivasan, R., Sorial, G.A., 2011. Treatment of taste and odor causing compounds 2-methyl isoborneol and geosmin in drinking water: a critical review. J. Environ. Sci 23, 1–13. https://doi.org/10.1016/s1001-0742(10)60367-1.

Steele, J.H., 1965. Notes on some theoretical problems in production ecology. In: Goldman, C.R. (Ed.), Primary Production in Aquatic Environments. University of California Press, Berkeley, CA.

Tang, C., Li, Y., Acharya, K., 2016. Modeling the effects of external nutrient reductions on algal blooms in hyper-eutrophic Lake Taihu, China. Ecol. Eng. 94, 164–173. https://doi.org/10.1016/j.ecoleng.2016.05.068.

Thomann, R.V., Mueller, J.A., 1987. Principles of Surface Water Quality Modeling and Control. Harper & Row Publishers.

Van Nieuwenhuyse, E.E., Jones, J.R., 1996. Phosphorus chlorophyll relationship in temperate streams and its variation with stream catchment area. Can. J. Fish. Aquat. Sci. 53, 99–105. https://doi.org/10.1139/f95-166.

Van Rijn, L.C., 1993. Principles of Sediment Transport in Rivers, Estuaries and Coastal Seas (Vol. 1006). Aqua publications, Amsterdam.

Willmott, C.J., 1981. On the validation of models. Phys. Geogr. 2 (2), 184–194. https://doi.org/10.1080/02723646.1981.10642213.

Willmott, C.J., 1984. On the Evaluation of Model Performance in Physical Geography, Spatial statistics and Models. Springer, pp. 443–460.

Wu, G., Xu, Z., 2011. Prediction of algal blooming using EFDC model: case study in the Daoxiang Lake. Ecol. Modell 222, 1245–1252. https://doi.org/10.1016/j.ecolmodel.2010.12.021.

Xia, R., Wang, G., Zhang, Y., Yang, P., Yang, Z., Ding, S., Jia, X., Yang, C., Liu, C., Ma, S., 2020. River algal blooms are well predicted by antecedent environmental conditions. Water Res. 185, 116221 https://doi.org/10.1016/j.watres.2020.116221.

Zhang, Y.S., Sonn, Y.G., Park, C.W., Hyun, B.K., Moon, Y.H., Song, K.C., 2011. Soil physical and chemical characteristics of river-bed sediments in river basins. Korean Soc. Soil Sci. Fertilizer 44, 963–969. https://doi.org/10.7745/KJSSF.2011.44.6.963.

Zhang, Z., Zimmermann, N.E., Calle, L., Hurtt, G., Chatterjee, A., Poulter, B., 2018. Enhanced response of global wetland methane emissions to the 2015–2016 El Niño-Southern oscillation event. Environ. Res. Lett. 13 (7), 074009 https://doi.org/10.1088/1748-9326/aac939.